

Tuning pGa with Chelating Agents Related to (*o*-Hydroxybenzyl)iminodiacetic Acid

Olivier Jarjayes^{*[a]} Florent Mortini,^[a] Amaury du Moulinet d'Hardemare,^[a]
Christian Philouze,^[a] and Guy Serratrice^[a]

Keywords: Carboxylate ligands / Gallium / N ligands / Potentiometry / Stability constants

Gallium complexes with R-(*o*-hydroxybenzyl)iminodiacetate ligands (**Lx**) have been synthesized and their thermodynamic constants determined in aqueous solution by potentiometric titration. These quantitative results were also confirmed by ¹H and ¹⁹F NMR spectroscopy. An X-ray study of Ga**L3** (R = NO₂) showed that the gallium(III) ion is hexacoordinate with two H₂O molecules in *cis* positions. The ability of the ligands

to chelate Ga^{III} was evaluated at physiological pH and ionic strength from the pGa values. Among the different ligands studied, **L6** (R = OMe) has a pGa value two orders of magnitude higher than that of the complex between Ga and the blood serum protein transferrin.

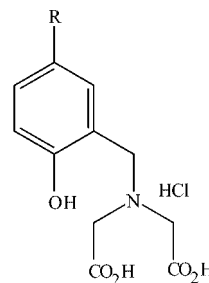
(© Wiley-VCH Verlag GmbH & Co. KGaA, 69451 Weinheim, Germany, 2005)

Introduction

The design and synthesis of new chelating agents for effective coordination of Ga^{III} has received an important and increasing interest in the past decade. This is in part because of promising potential applications of ⁶⁷Ga and ⁶⁸Ga complexes as diagnostic radiopharmaceuticals.^[1–4] In order to be considered as radiopharmaceuticals, these metal complexes must be stable with respect to demetalation by the blood serum protein transferrin and they must have a conditional stability constant greater than that of Ga–transferrin.^[5] Moreover, the presence on the ligand of a second functional group that is not involved in the metal chelating process leads to a bifunctional chelator^[6] and allows covalent linkage to targeting biomolecules such as antibodies, small proteins, or synthetic macromolecules. These conjugates are considered as *in vivo* metal carriers. Concerning the metal bonding unit, a large number of chelators have been synthesized and studied,^[6] including groups such as catechols, hydroxamates, hydroxypyridinones, or aminophosphonates. Among them, aminocarboxylate groups presenting a high affinity towards Ga^{III} have been widely used to build polydentate ligands based on EDTA and DTPA backbones. However, ligands possessing both aminocarboxylate and phenolic sub-units have been studied to a lesser extent, even though they present the highest stability constants towards Ga^{III} [for HBED, i.e. *N,N'*-bis(2-hydroxybenzyl)ethylenediamine-*N,N'*-diacetic acid, log β_{110} = 37.7].^[7] The introduction of a conjugation group for the

attachment to a biomolecule is rather difficult when several phenolic rings are present.^[8,9] For this reason, we have reported the synthesis of bifunctional chelating agents based on phenol. This synthesis compares favorably in terms of simplicity and step saving with other bifunctional structures based on DTPA or DOTA. Moreover, a wide number of chemical functions can be made available in the *para* position of the phenol.

In this present work, we report the stability constants of the gallium complexes in aqueous solution with R-(*o*-hydroxybenzyl)iminodiacetate ligands (**Lx**; Figure 1) to determine if these systems are good candidates for radiopharmaceutical applications. These studies were performed by combining potentiometry and NMR (¹H and ¹⁹F) spectroscopy. Solid-state characterizations were also performed for **L6** (R = OMe) and the complex Ga**L3** (R = NO₂).



[a] Laboratoire d'Etudes Dynamiques et Structurales de la Sélectivité, Université Joseph Fourier, Grenoble 1, UMR 5616, ICMG FR CNRS 2607, BP 53, 38041 Grenoble Cedex 09, France
Fax: +33-4-7651-4927
E-mail: Olivier.Jarjayes@ujf-grenoble.fr

R	Me	CHO	NO ₂	CH ₂ OH	F	OMe	H
Lx	L1	L2	L3	L4	L5	L6	HBIDA

Figure 1. Structure of the ligands **Lx**.

Results and Discussion

Synthesis of the Ligands and Complexes

The **Lx** ligands are easily accessible from the appropriate *para*-substituted phenols and diethyl iminodiacetate in a solvent-less Mannich reaction, followed by the hydrolysis of the diethyl ester functions with hydrochloric acid. More details concerning the ligands' synthetic procedure have been described elsewhere.^[10]

Solid-State Structure of the Ligand **L6** and Complex **GaL3**

Crystals of **L6** ($R = \text{OMe}$) suitable for X-ray structure determination were obtained from an aqueous solution (10^{-2} M, pH 2.8) stored at room temperature. Details of the data collections are summarized in Table 4. The unit cell of **L6** is depicted in Figure 2 and the structural representation of **L6** is given in Figure 3.

The unit cell is shown down the a axis and displays two molecules, one of which is linked to three molecules of neighboring cells through hydrogen bonds ($\text{O5-H4}\cdots\text{O5}^* = 1.22 \text{ \AA}$, $\text{O3-H3}\cdots\text{O3}^* = 1.21 \text{ \AA}$, $\text{O1-H1}\cdots\text{O2}^* = 1.95 \text{ \AA}$). This representation explains the zwitterionic state of **L6**, since two hydrogens atoms (**H3** and **H4**) of the molecule are shared with two molecules from adjacent unit cells. There is also a hydrogen bond between the hydrogen **H1** of the phenol and the oxygen **O2**^{*} of the carboxylic function. All of these intermolecular hydrogen bonds provide the stability of the crystal. In addition, three intramolecular hydrogen bonds are observed ($\text{N1-H2}\cdots\text{O2} = 2.18 \text{ \AA}$, $\text{N1-H2}\cdots\text{O4} = 2.23 \text{ \AA}$, $\text{N1-H2}\cdots\text{O1} = 2.56 \text{ \AA}$; see Figure 2). They realise the cohesion of the internal structure of the molecule, and might propitiously orientate the donor atoms for complexation.

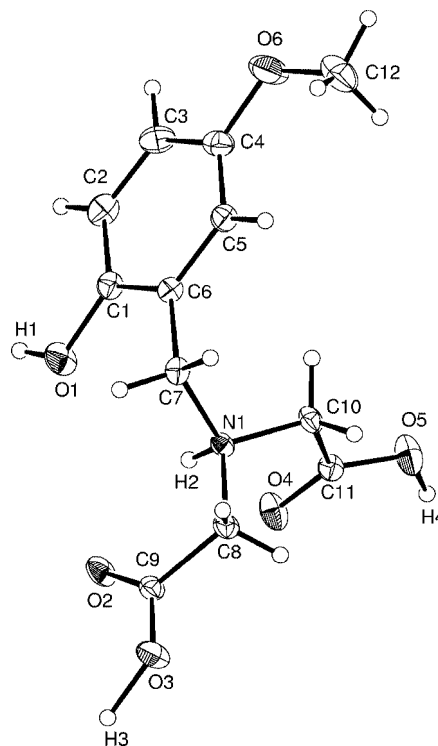


Figure 3. Structural representation of **L6**.

Among the different **GaLx** complexes, only **GaL3** gave suitable crystals for an X-ray structural study. The ORTEP diagram of **GaL3** ($R = \text{NO}_2$) is depicted in Figure 4, with selected bond lengths and angles listed in Table 1.

The gallium ion is located in a slightly distorted octahedral coordination environment formed by the deprotonated phenolic oxygen, two carboxylate oxygen atoms, the tertiary nitrogen atom, and two H_2O molecules coordinated in *cis* positions. The bond lengths of Ga to the tertiary amino

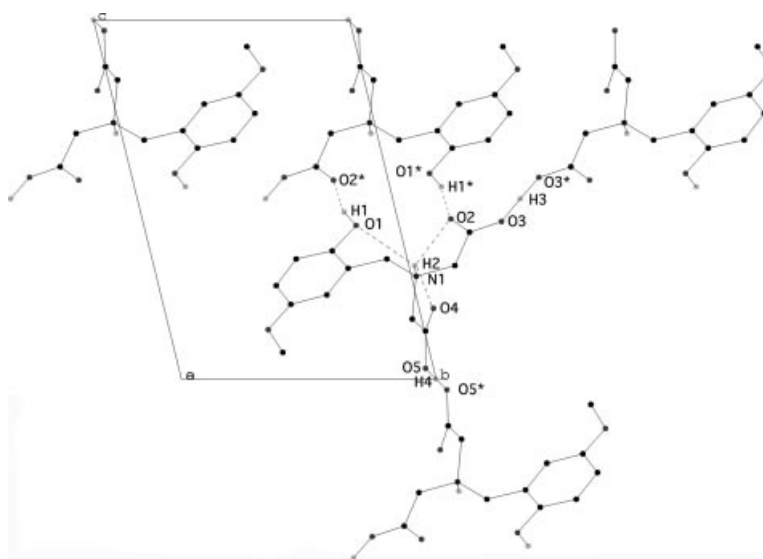


Figure 2. Unit cell representation down the a axis. This representation explains the zwitterionic state of **L6** as it can be seen that two protons of the molecule are shared with two molecules from adjacent unit cells (most of the hydrogen atoms have been omitted for clarity).

Table 1. Selected bond lengths [Å] and angles [°] for GaL3.

Ga–O(1)	1.884(2)	Ga–O(3)	2.077(2)	Ga–O(5)	1.938(1)
Ga–O(8)	1.964(2)	Ga–O(9)	1.956(2)	Ga–N(1)	2.097(2)
O(1)–Ga–O(3)	170.88(7)	O(1)–Ga–O(5)	95.87(7)	O(1)–Ga–O(8)	88.94(7)
O(1)–Ga–O(9)	97.78(7)	O(1)–Ga–N(1)	94.86(7)	O(3)–Ga–O(5)	88.91(7)
O(3)–Ga–O(8)	87.04(7)	O(3)–Ga–O(9)	90.23(7)	O(3)–Ga–N(1)	77.76(7)
O(5)–Ga–O(8)	172.97(7)	O(5)–Ga–O(9)	86.75(6)	O(5)–Ga–N(1)	85.24(6)
O(8)–Ga–O(9)	87.53(7)	O(8)–Ga–N(1)	99.49(7)	O(9)–Ga–N(1)	165.66(7)

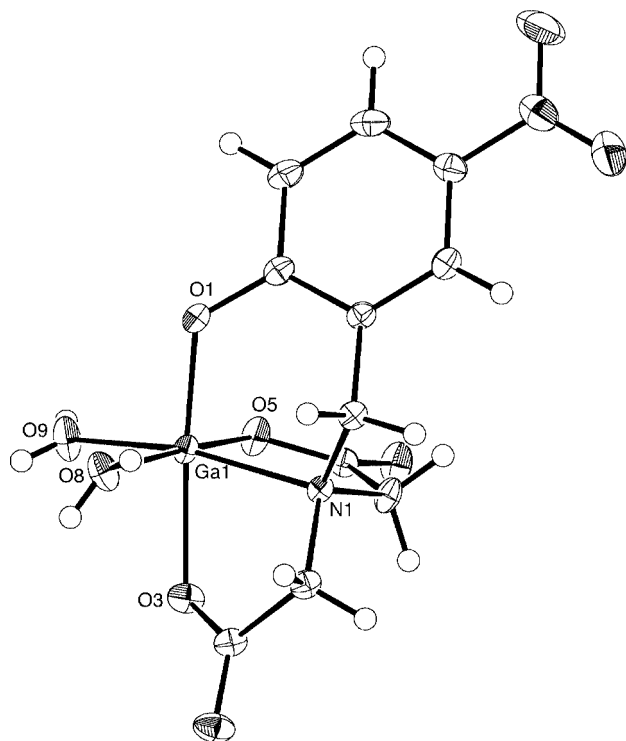


Figure 4. Structural representation of GaL3.

nitrogen atom and to the carboxylate oxygen atoms presented in Table 1 are consistent with those observed in complexes obtained with other carboxylate ligands.^[11,12] The gallium–phenolate bond length (1.884 Å) compares well with such bonds in other similar complexes,^[13] but is significantly shorter than that found for the bridging phenolate in [Ga₂(HXTA)] [1.999 Å and 2.078 Å;^[14] HXTA = *N,N'*-

(2-hydroxy-5-methyl-1,3-xylylene)bis(*N*-methoxycarbonyl)glycine].^[15] The N(1)–Ga–OOC angles have the largest deviation from 90°, probably caused by the steric constraints of the five-membered chelate rings.

Ligand Deprotonation Constants

The deprotonation constants, K_{an} , of the ligands (as hydrochloride salts) investigated in this work were studied by potentiometric titrations. Analysis of the titration curve (part a of Figure 5, as an example) by the program SUPERQUAD^[16] yielded the pK_{an} values defined by Equations (1) and (2) and reported in Table 2.

$$LH_n \rightleftharpoons LH_{n-1} + H^+ \quad (1)$$

$$K_{an} = [LH_{n-1}][H^+]/[LH_n] \quad (2)$$

For each ligand, three pK_a values out of the four possible ones were determined, corresponding to one carboxylic acid group, the ammonium group, and the phenolic hydroxyl group. The pK_a value of the other carboxylic acid was inferred to be significantly lower than 2, since if we tried to include this pK_a in the fit, this constant was discarded by the program. The pK_a values for the different **Lx** ligands are close to those given (see Table 2) for the ligand HBIDA [*N*-(2-hydroxybenzyl)iminodiacetic acid],^[17,18] which has a similar structure.

From a general point of view, it should be noted that the substituent in the *para* position of the phenol plays an important part in its acidity. For example, the presence of an electron-withdrawing group for **L2** (R = CHO) and **L3** (R = NO₂) increases the phenol acidity (pK_{a1} = 10.35 and 10.05, respectively, instead of 11.7 for HBIDA). In the same way, the phenolate basicity of **L1** (R = Me) is slightly higher

Table 2. Deprotonation constants of the ligands **Lx**.

$pK_{an}^{[a]}$	L1	L2	L3	L4	L5	L6	HBIDA ^[b]
pK_{a1}	12.1(1) ^[c]	10.35(2)	10.05(5) 10.22 ^[c]	12.2(1) ^[c]	12.3 ^[d]	12.5 ^[g]	11.7
pK_{a2}	8.30(1) 8.0 ^[f]	6.65(6)	6.20(4) 6.18 ^[e]	8.05(9)	7.60(7) 7.5 ^[d]	7.92(5)	8.07
pK_{a3}	2.3(1) ^[c]	2.1(1) ^[c]	2.4 ^[c]	1.9 ^[f]	1.8 ^[d]	1.9 ^[f]	2.34

[a] All values were determined at 25 °C and $I = 0.1$ M. Values in parentheses are standard deviations in the last significant digit. [b] *N*-(2-Hydroxybenzyl)iminodiacetic acid.^[17] [c] Estimated value since the true uncertainty in these pK_a values is greater than the standard deviation obtained from the least-squares fitting of the potentiometric data. [d] Determined by ¹⁹F NMR spectroscopy. [e] Ref.^[18] [f] Determined by ¹H NMR spectroscopy. [g] Determined by UV/Vis spectroscopy.

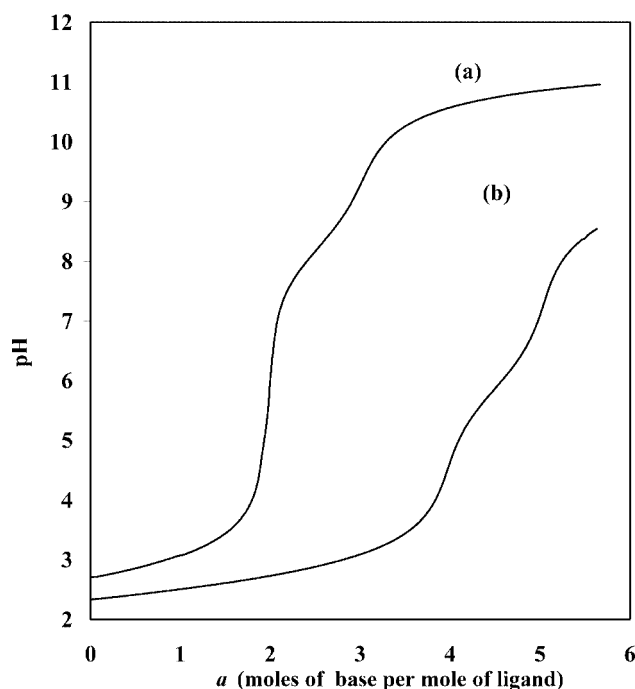


Figure 5. Potentiometric titration curves for (a) 1 mM ligand **L1** and (b) **L1** + Ga^{3+} (1:1, 1 mM). a = mols of base added per mol of ligand. All solutions were at 25 °C and $I = 0.1$ M (NaNO_3). The data were refined with the program SUPERQUAD ($\sigma_{\text{fit}} = 3.5\text{--}4.5$).

than that of HBIDA; this effect is due to the presence of the methyl group, which increases the electronic density on the phenolic ring. The effect of these groups also has an influence on the ammonium acidity, which is more acidic for ligands **L2** and **L3** ($\text{p}K_{\text{a}2}$ values of 6.65 and 6.21, respectively). On the other hand, for ligands **L1** and **L4**, which bear low inductive groups ($\text{R} = \text{Me}$ and CH_2OH , respectively), or with an electron-donating group ($\text{R} = \text{OMe}$, **L6**), the ammonium always has a $\text{p}K_{\text{a}}$ value larger than 8.

Since low $\text{p}K_{\text{a}}$ values are difficult to determine by potentiometric titration, some of the deprotonation constants of **L4** and **L6** were also calculated by ^1H NMR spectroscopy from the titration curves of δ vs. pH under the same conditions of ionic strength as used for the potentiometric study (Table 3). The K_{an} values were obtained from the chemical shift.^[19] The resonances of the methylene protons of the benzylic and acetic (CH_2COO) positions (singlets) become more shielded upon addition of base ($\Delta\delta = 0.8$ ppm in all the cases for pH ranging from 0.5 to 12) while the deprotonations only produce a small chemical shift (around 0.1 ppm) of the three aromatic protons. These observations make it clear that these protons are sensitive to the protonation state of the amine and one of the two carboxylic functions. In the same way, ^{19}F NMR spectroscopy can be considered as an excellent tool for the $\text{p}K_{\text{a}}$ determination for **L5** because three constants out of the four can be determined. The fourth deprotonation produces a marked change in the ^{19}F chemical shift ($\Delta\delta = 6$ ppm). This increased shielding of the fluorine ring substituent indicates a net increase of negative charge on the aromatic ring in this process. This observation is consistent with the

loss of the phenolic proton, which cannot be determined by ^1H NMR spectroscopy. It is also very interesting to notice that the fluorine atom is a much more sensitive probe than ^1H , since a carboxylic function located in a 9J position can affect the fluorine chemical shift. The agreement between the values from various experimental techniques is reasonable, and the dissociation constants correlate well with the data reported for HBIDA (see Table 2).

Table 3. Stability constants and pGa values.

Con- stants ^[a]	L1	L2	L3	L4	L5	L6	HBIDA ^[b]
$\log \beta_{110}^{\text{GaLx}}$	23.5	20.5	20.1	22.5	22.4	25.3	21.40
$\log \beta_{110}^{\text{GaLx}}$	22.1	19.4	19.1	21.1	21.4	25.2	21.55
$\text{p}K_{\text{OH}}^{\text{Lx}}$ ^[c]	5.70(4)	5.77(2)	5.54(2)	5.72(6)	6.21(3)	6.42(1)	5.75
	5.3 ^[d]				6.0 ^[e]		
$\text{p}K_{\text{OH}}^{\text{Lx}}$ ^[f]	8.2(1)				8.8(1)		8.53
					8.8 ^[f]		
pGa ^[g]	19.1	19.0	19.2	18.2	18.3	21.5	19.1

[a] All values were determined at 25 °C and $I = 0.1$ M (NaNO_3). [b] Ref.^[17] [c] $K_{\text{OH}}^{\text{Lx}} = [\text{GaLx}(\text{OH})][\text{H}^+]/[\text{GaLx}]$ for the equilibrium $\text{GaLx} + \text{H}_2\text{O} \rightleftharpoons \text{GaLx}(\text{OH}) + \text{H}^+$. [d] Determined by ^1H NMR titration. [e] Determined by ^{19}F NMR titration. [f] $K_{\text{OH}}^{\text{Lx}} = [\text{GaLx}(\text{OH})_2][\text{H}^+]/[\text{GaLx}(\text{OH})]$ for the equilibrium $\text{GaLx}(\text{OH}) + \text{H}_2\text{O} \rightleftharpoons \text{GaLx}(\text{OH})_2 + \text{H}^+$. [g] Calculated for $[\text{Lx}]_{\text{tot}} = 10^{-5}$ M and $[\text{Ga}]_{\text{tot}} = 10^{-6}$ M at pH 7.4.

Stability Constants of the Gallium Complexes

It was not possible to determine the stability constants $\beta_{110}^{\text{GaLx}}$ of the complexes by potentiometric titration since the formation of the complexes is complete at low pH values (Figure 5b). The titration curves for a 1:1 ratio of Ga^{III} and ligand (Figure 5b as an example) exhibit two breaks at $a = 4$ and $a = 5$, where a is equal to the number of mols of base added per mol of ligand. This indicates the formation of the hydroxo complexes $[\text{GaLx}(\text{OH})]$ and $[\text{GaLx}(\text{OH})_2]$ at relatively low pH values. Analysis of the titration curves with the program SUPERQUAD^[16] yielded the $K_{\text{OH}}^{\text{Lx}}$ ($n = 1$ or 2) constants expressed by Equation (3).

$$K_{\text{OH}}^{\text{Lx}} = [\text{GaLx}(\text{OH})_n][\text{H}^+]/[\text{GaLx}(\text{OH})_{n-1}] \quad (3)$$

The $K_{\text{OH}}^{\text{Lx}}$ values are given in Table 3, and can also be determined by ^1H NMR spectroscopy for **GaL1**. In the case of **GaL5**, ^{19}F NMR spectroscopy was used to determine the two hydrolysis constants, as shown in Figure 6, revealing two important chemical shift jumps ($\Delta\delta = 0.75$ and 1.2 ppm) as a function of pH.

The obtained values are in good agreement with the potentiometric titrations. It should be noted that higher $\text{p}K_{\text{OH}}^{\text{Lx}}$ values have been obtained for **GaL5** and **GaL6** in relation with the higher basicity of the phenolate group as it increases the electronic density on the metal ion. The stability constants $\beta_{110}^{\text{GaLx}}$ were determined in acidic medium^[19] (pH 2.01) by metal–metal competition, using the absorbance of **FeLx** as a spectral probe. In these experiments, exchange of Ga^{III} with Fe^{III} was allowed to occur [Equations (4) and (5)].

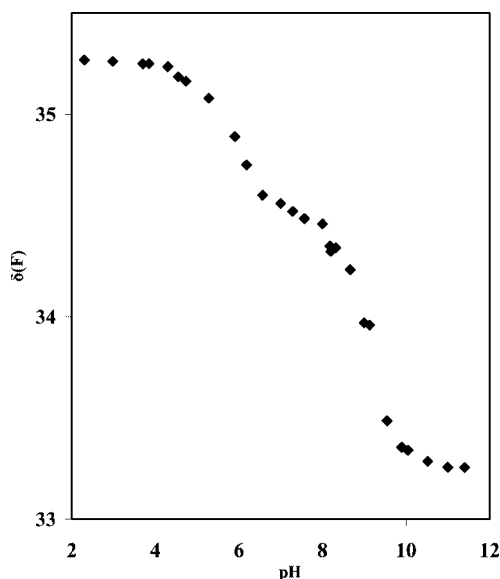


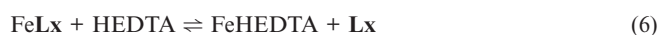
Figure 6. Dependence of the ^{19}F chemical shift (vs. C_6F_6) of GaL5 on the addition of NaOH [measured in an $\text{H}_2\text{O}/\text{D}_2\text{O}$ (80:20) medium at 25°C and $I = 0.1 \text{ M NaNO}_3$].



$$K = \frac{[\text{GaLx}][\text{Fe}^{\text{III}}]}{[\text{FeLx}][\text{Ga}^{\text{III}}]} = \frac{\beta_{110}^{\text{GaLx}}}{\beta_{110}^{\text{FeLx}}} \quad (5)$$

The amount of uncomplexed Lx was assumed to be negligible.

Knowledge of the formation constants of FeLx complexes, along with mass balance, absorbance, and pH measurements, is necessary to calculate the formation constants of GaLx . Beforehand, the stability constants of FeLx ($\beta_{110}^{\text{FeLx}}$) were determined by competition experiments against HEDTA^[17] over the pH range 2–2.5. The following equation corresponds to the equilibrium [charges omitted for clarity, Equation (6)].



where HEDTA is (hydroxyethyl)ethylenediaminetriacetic acid [Equation (7)].

$$K' = \frac{[\text{Lx}][\text{FeHEDTA}]}{[\text{FeLx}][\text{HEDTA}]} = \frac{\beta_{110}^{\text{FeHEDTA}}}{\beta_{110}^{\text{FeLx}}} \quad (7)$$

The concentrations of FeLx complexes were calculated from the absorbances between 486 and 578 nm (depending on the ligand Lx), where FeLx is the only absorbing species. The concentration of the other species was calculated from mass balance equations and pH, using the usual α Ringbom coefficient.^[21] With the known formation constant of Fe^{III} -HEDTA ($\log \beta_{110}^{\text{FeHEDTA}} = 19.8$), and the deprotonation constants of HEDTA ($\text{p}K_{\text{a}1} = 9.81$, $\text{p}K_{\text{a}2} = 5.37$, and $\text{p}K_{\text{a}3} = 2.6$),^[18] the values of $\beta_{110}^{\text{FeLx}}$ and $\beta_{110}^{\text{GaLx}}$ were calculated from Equations (6) and (7), respectively, and are reported in Table 3. They span over the range 19.1–25.3 and are consistent with the one obtained for the HBIDA ligand taken as the reference (no electronic effect).^[17]

As we can observe, the stability of the complexes (Fe^{III} or Ga^{III}) increases with the basicity of the phenolate, i.e. with its greater electron donor ability. Ligands with an electron-withdrawing substituent (the more acidic) lead to complexes with a gallium stability constant lower than that of Ga-transferrin ($\log K = 19.8$),^[22] whereas ligands with electron-donating substituents ($\text{R} = \text{OMe}$, Me) give $\beta_{110}^{\text{GaLx}}$ values up to five times higher than the complex Ga-transferrin . The distribution curves shown in Figure 7 for the 1:1 $\text{Ga}^{\text{III}}:\text{L1}$ system provide a typical picture of the successive complexes formed as a function of pH. GaL1 is dominant in the pH range 2–4.5, while the first hydroxo complex $[\text{GaL1}(\text{OH})]$ is the major species at physiological pH. $\text{p}K_{\text{OH}}^1$ values can also be related to the basicity of the phenolate group: this increases the electronic density on the metal ion and decreases its affinity towards coordinated water molecules, so the highest $\text{p}K_{\text{OH}}^1$ values are obtained for GaL5 and GaL6 .

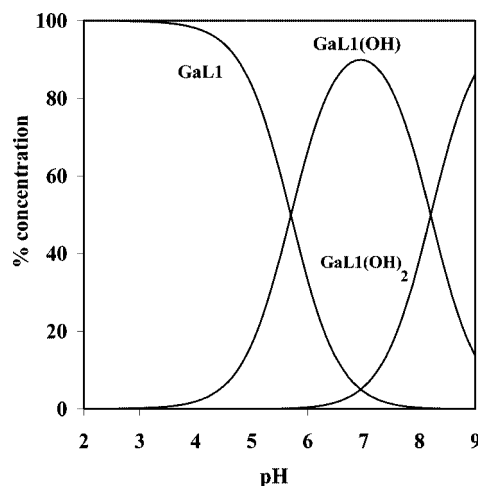


Figure 7. Distribution curves for the system $\text{Ga}^{\text{III}}\text{--L1}$ as a function of pH. $[\text{Ga}^{3+}] = 1 \text{ mM}$ and $[\text{L1}] = 10 \text{ mM}$.

Since the ligands are weak acids, proton competition occurs depending on their $\text{p}K_{\text{a}}$ and the pH. The pGa ($-\log [\text{Ga}^{3+}]$) is thus a better measure of the relative complexation efficiency of the ligands under given conditions of pH, Ga , and Lx concentrations: the larger the pGa values, the more effective the ligand. The pGa values for pH 7.4 ($[\text{Ga}^{3+}] = 10^{-6} \text{ M}$, $[\text{Lx}] = 10^{-5} \text{ M}$) are collected in Table 3. They have also been calculated for pH values over the range 2–8 and reported as the plot $\text{pGa} = f(\text{pH})$ presented in Figure 8. In this pH range, the uncertainty in the high $\text{p}K_{\text{a}}$ values does not affect the calculations of the pGa values.

Except for L6 , it is important to note a similar efficiency in the complexation of Ga^{III} by the various aminophenolate ligands. pGa values have small variations whenever Lx bears electron-withdrawing substituents ($\text{R} = \text{CHO}$, $\text{R} = \text{NO}_2$) or an electron-donating group ($\text{R} = \text{Me}$). These ligands' complexing abilities are thus similar to Ga-EDTA ($\text{pGa} = 20.0$)^[22] and Ga-DTPA ($\text{pGa} = 20.2$)^[22] but with a lower denticity. pGa vs. pH curves indicate that L6 is the best complexing agent of this family over the whole pH range

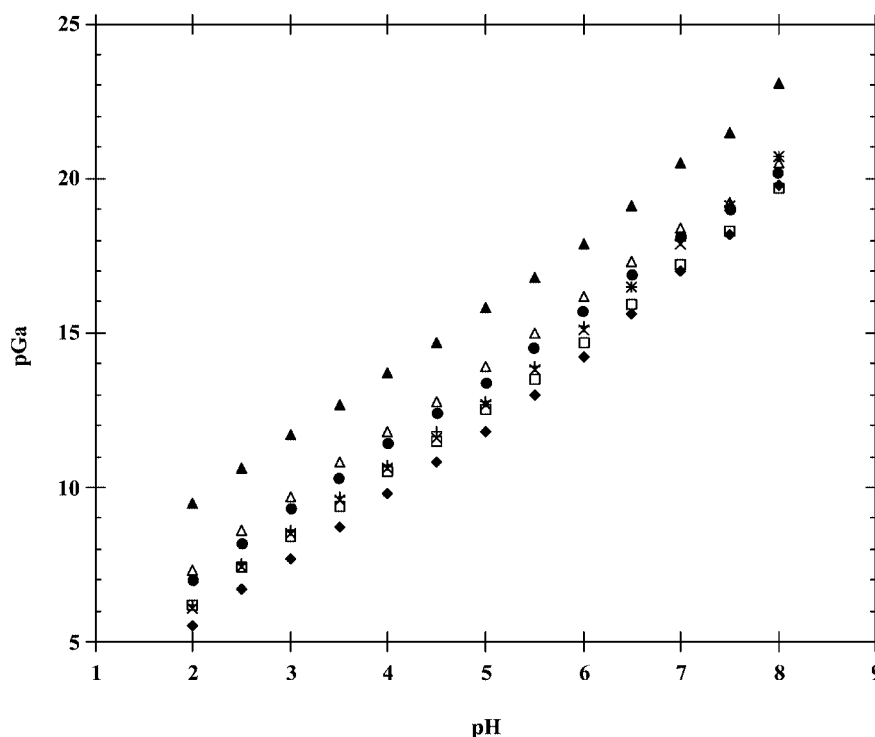


Figure 8. Plot of pGa ($-\log [\text{Ga}^{3+}]$) vs. pH. pGa was calculated for $[\text{Lx}] = 10^{-5} \text{ M}$ and $[\text{Ga}^{3+}] = 10^{-6} \text{ M}$. For HBIDA, the deprotonation constants and the complexation constants β_{110} were taken from ref.^[20] (\times L1, \bullet L2, Δ L3, \blacklozenge L4, \square L5, \blacktriangle L6, $+$ HBIDA).

(pGa = 21.5 at pH 7.4). This good affinity is due to an increased basicity of the phenolate with a methoxy group in the *para* position. Indeed, according to Pearson's principle of hard and soft acids and bases (HSAB),^[23] a very basic negative oxygen donor has a high affinity for a hard metal ion such as Ga^{III} . Except for L6, and as could be expected from theory, acidic ligands (those bearing electron-withdrawing substituents) have the best complexing ability at low pH. So, L6 is a good Ga^{III} chelator compared to the Ga-transferrin (pGa = 19.7)^[22] system (around two orders of magnitude difference). GaL6 may thus be resistant to demetalation *in vivo*, and radiopharmaceutical applications are possible in this context.

Conclusions

This work has shown that the R-(*o*-hydroxybenzyl)iminodiacetate ligands (obtained in only two steps) with a potential conjugating group in the *para* position to the phenol and a rather low denticity are strong chelators for Ga^{III} . For the GaL3 (R = NO_2) complex in the solid state, the Ga^{III} ion is hexacoordinate with two water molecules in *cis* positions. The protonation constants of the ligands and the hydroxo complexes' formation constants were measured by different techniques and gave consistent data. Considering the pGa values, GaL6 (R = OMe) appears to be a promising candidate for use in radioimaging since the stability constant of Ga-transferrin is two orders of magnitude lower. Studies with $^{67/68}\text{Ga}$ radiolabeling are now in progress in order to confirm the kinetic inertness of these bi-

functional chelating systems against common decomplexation pathways.

Experimental Section

General Remarks: ^1H NMR spectra were recorded on a Bruker AC 200 spectrometer. Chemical shifts are reported in ppm from internal sodium 3-(trimethylsilyl)propane-1-sulfonate. ^{19}F NMR spectra were recorded on a Varian U400 with chemical shifts in ppm relative to an external C_6F_6 reference in CDCl_3 ($\delta = -163$ ppm relative to CFCl_3). The pH was adjusted with small additions of concentrated HCl or NaOH solutions (prepared in D_2O). The pK_a values were measured in pure D_2O and the pD was obtained from the pH meter readings by adding 0.4 units.^[24] For the dissociation constants in D_2O and H_2O , the relationship $\text{pK}_D = 1.018 \text{pK}_H + 0.43$ was used.^[25] Measurements were made in a $\text{H}_2\text{O}/\text{D}_2\text{O}$ medium (80:20 v/v) and in this case no correction for isotopic or solvents effects was needed. Analyses were performed by the Service Central d'Analyse (CNRS Solaize). All chemicals were obtained from Acros or Aldrich and were used without further purification.

Synthesis of GaL3: 10 mL of an aqueous solution of NaOH (2 mmol) was added to a solution of L3 (165 mg, 0.5 mmol) in water (10 mL). The gallium nitrate salt in H_2O (0.5 mmol in 10 mL) was then added to this homogeneous solution and the pH adjusted to 3–4. After stirring for 30 min, half of the solvent was slowly removed under reduced pressure. Slow concentration of the filtrate over a period of one week yielded suitable crystals for X-ray diffraction studies. Yield: 164 mg (81%). $\text{C}_{11}\text{H}_{15}\text{GaN}_2\text{O}_{10}$: calcd. C 32.62, H 3.73, Ga 17.22, N 6.92; found C 32.82, H 3.59, Ga 16.95, N 6.85. ^1H NMR (DMSO): $\delta = 3.16\text{--}3.38$ (dd, $J = 21$ Hz, 4 H, H_{ac}), 3.95 (s, 2 H, H_{benz}), 6.65–6.67 (d, $J = 6$ Hz, 1 H, H_{ar}), 7.95–8.05 (m, 2 H, H_{ar}) ppm.

Table 4. Summary of crystallographic data for **L6** and **GaL3**.

	L6	GaL3
Formula	C ₁₂ H ₁₅ NO ₆	C ₁₁ H ₁₃ GaN ₂ O ₉
<i>M</i>	269.25	386.95
Symmetry	triclinic	monoclinic
Morphology	pale yellow prism	pale yellow prism
Crystal dimensions [mm]	32 × 21 × 14	35 × 22 × 20
<i>a</i> [Å]	5.459(5)	6.9456(3)
<i>b</i> [Å]	9.268(4)	32.120(1)
<i>c</i> [Å]	12.902(3)	6.9606(2)
<i>α</i> [°]	103.97(3)	90
<i>β</i> [°]	93.58(4)	117.7(1)
<i>γ</i> [°]	78.52(5)	90
Unit-cell volume [Å ³]	620.7(6)	1374.9(7)
<i>T</i> [K]	293.0	293.0
Space group	<i>P</i> $\bar{1}$	<i>P</i> 2 ₁ / <i>a</i>
<i>Z</i>	2	4
Diffractometer	Enraf–Nonius CAD-4	Enraf–Nonius Kappa CCD
Monochromator	graphite	graphite
Radiation (wavelength)	Mo- <i>K</i> _α (0.71073 Å)	Mo- <i>K</i> _α (0.71073 Å)
<i>μ</i> [mm ^{−1}]	0.116	2.055
No. of reflections (measured)	3756	20881
No. of reflections (unique)	3609	6097
No. of reflections	1981 [<i>I</i> > 2.6σ(<i>I</i>)]	2955 [<i>I</i> > 3.0(<i>I</i>)]
<i>R</i> _{int}	0.028	0.062
<i>R</i>	0.053	0.038
<i>R</i> (<i>w</i>)	0.056	0.038

Potentiometric Titrations: All the measurements were made at 25 °C and the solutions were prepared with deionized water that had been distilled twice. The ionic strength was fixed at *I* = 0.1 M with NaNO₃ (PROLABO puriss). The potentiometric titrations were performed using an automatic titrator system, DMS 716 Titrino (Metrohm), equipped with a combined glass electrode (Metrohm, filled with saturated NaCl solution) and connected to an IBM Aptiva microcomputer. The electrodes were calibrated to read pH according to the classical method^[26] (from titration of 0.01 M HClO₄ with 0.025 M NaOH). The ligands and their gallium(III) complexes (ca. 0.001 M) were titrated with standardized 0.025 M sodium hydroxide. Argon was bubbled through the solutions to exclude CO₂ and O₂. Aqueous sodium hydroxide (0.1 M NaOH) was prepared from 1 M commercial NaOH solution (Prolabo) and was standardized against hydrogen phthalate solution. The titration data (120 points collected over the pH range 2.5–10.5 for the ligand solutions and 100 points collected over the pH range 2.5–10 for the Ga^{III}–ligand solution) were refined with the nonlinear least-squares refinement program SUPERQUAD^[16] to determine the deprotonation constants (σ_{fit} in the range 3.5–4.5). The p*K*_{an} values were calculated from the cumulative constants determined with the above program. The uncertainties in the p*K*_{an} values correspond to the standard deviations (1σ) in the cumulative constants.

Spectrophotometric Experiments: UV/Vis absorption spectra were recorded with a Perkin–Elmer Lambda 2 spectrometer using 1-cm path-length quartz cells and connected to a microcomputer; the acquisition was made with the UV Winlab software (Perkin–Elmer). The temperature was maintained at 25 °C with a Perkin–Elmer PTP.1 variable temperature unit. The pH measurements were made with a 713 Metrohm digital pH meter equipped with a micro-electrode. The ionic strength was fixed at *I* = 0.1 M with NaNO₃.

X-ray Crystallographic Data Collection and Refinement of the Structures: The main crystallographic features, the strategy used for the crystal structure determination, and its results are gathered in Table 4. Data collection was performed at room temperature. The

*U*_{iso} of the H atoms was fixed to 1.2 *U*_{eq} of the C atom to which they are bound. All the structures were solved by direct methods (SIR92).^[27]

CCDC-201447 (for **L6**) and -201562 (for **GaL3**) contain the supplementary crystallographic data for this paper. These data can be obtained free of charge from The Cambridge Crystallographic Data Centre via www.ccdc.cam.ac.uk/data_request/cif.

- [1] S. Jurisson, D. Berning, W. Jia, D. Ma, *Chem. Rev.* **1993**, 93, 1137–1156.
- [2] J. Burgess, *Chem. Soc. Rev.* **1996**, 25, 85–92.
- [3] C. J. Anderson, M. J. Welch, *Chem. Rev.* **1999**, 99, 2219–2234.
- [4] E. Arslantas, P. M. Smith-Jones, G. Ritter, R. R. Schmidt, *Eur. J. Org. Chem.* **2004**, 19, 3979–3984.
- [5] W. R. Harris, L. Messori, *Coord. Chem. Rev.* **2002**, 228, 237–362.
- [6] S. Liu, D. S. Edwards, *Bioconjugate Chem.* **2001**, 12, 7–34.
- [7] R. J. Motekaitis, Y. Sun, A. E. Martell, M. J. Welch, *Inorg. Chem.* **1991**, 30, 2737–2740.
- [8] C. J. Mathias, Y. Sun, J. M. Connnett, G. W. Philpott, M. J. Welch, A. E. Martell, *Inorg. Chem.* **1990**, 29, 1475–1480.
- [9] C. J. Mathias, Y. Sun, M. J. Welch, J. M. Connnett, G. W. Philpott, A. E. Martell, *Bioconjugate Chem.* **1990**, 1, 204–211.
- [10] A. du Moulinet d'Hardemare, O. Jarjays, F. Mortini, *Synth. Commun.* **2004**, 34, 3975–3988.
- [11] B. Achour, J. Costa, R. Delgado, E. Garrigues, C. F. G. C. Geraldes, N. Korber, F. Nepveu, M. I. Prata, *Inorg. Chem.* **1998**, 37, 2729–2740.
- [12] W. Niu, E. H. Wong, G. R. Weisman, Y. Peng, C. J. Anderson, L. N. Zakharov, J. A. Golen, A. L. Rheingold, *Eur. J. Inorg. Chem.* **2004**, 16, 3310–3315.
- [13] S. Liu, S. J. Rettig, C. Orvig, *Inorg. Chem.* **1992**, 31, 5400–5407.
- [14] O. Jarjays, A. du Moulinet d'Hardemare, A. Durif, M. T. Averbuch-Pouchot, *Acta Crystallogr., Sect. C* **1998**, 54, 931–933.
- [15] B. P. Murch, F. C. Bradley, P. D. Boyle, V. Papaefthymiou, L. Que Jr., *J. Am. Chem. Soc.* **1987**, 109, 7993–8003.
- [16] P. Gans, A. Sabatini, A. Vacca, *J. Chem. Soc., Dalton Trans.* **1985**, 6, 1195–2000.

- [17] W. R. Harris, R. J. Motekaitis, A. E. Martell, *Inorg. Chem.* **1975**, *14*, 974–978.
- [18] A. E. Martell, R. M. Smith, *Critical Stability Constants*, Plenum Press, New York, **1974**.
- [19] G. Serratrice, A. Zeghli, C. G. Béguin, G. Gellon, P. Baret, J. L. Pierre, *J. Chim. Phys.* **1992**, *89*, 549–557.
- [20] W. R. Harris, A. E. Martell, *Inorg. Chem.* **1976**, *15*, 713–720.
- [21] A. Ringbom, *Complexation*, in *Analytical Chemistry*, Intersciences, New York, **1963**.
- [22] Y. Sun, C. J. Anderson, T. S. Pajean, D. E. Reichert, R. D. Hancock, R. J. Motekaitis, A. E. Martell, M. J. Welch, *J. Med. Chem.* **1996**, *39*, 458–470.
- [23] R. G. Pearson, *Surv. Prog. Chem.* **1967**, *5*, 1–52.
- [24] P. K. Glasoe, F. A. Long, *J. Phys. Chem.* **1960**, *64*, 188–190.
- [25] H. J. C. Yeh, K. L. Kirk, L. A. Cohen, J. S. Cohen, *J. Chem. Soc., Perkin Trans. 2* **1975**, 928–932.
- [26] A. E. Martell, R. J. Motekaitis, *Determination and Use of Stability Constants*, 2nd ed., VCH Publishers, New York, **1992**.
- [27] A. Altomare, A. Cascarano, G. Giacovazzo, A. Guagliardi, *J. Appl. Crystallogr.* **1993**, *26*, 343–350.

Received: December 17, 2004

Published Online: September 15, 2005